World Journal of Diabetes

Submit a Manuscript: https://www.f6publishing.com

World J Diabetes 2021 May 15; 12(5): 658-672

DOI: 10.4239/wjd.v12.i5.658

ISSN 1948-9358 (online)

ORIGINAL ARTICLE

Basic Study

Diabetes-related intestinal region-specific thickening of ganglionic basement membrane and regionally decreased matrix metalloproteinase 9 expression in myenteric ganglia

Nikolett Bódi, Diána Mezei, Payal Chakraborty, Zita Szalai, Bence Pál Barta, János Balázs, Zsolt Rázga, Edit Hermesz, Mária Bagyánszki

ORCID number: Nikolett Bódi 0000-0002-9774-1387; Diána Mezei 0000-0002-6343-4485; Payal Chakraborty 0000-0001-5471-2888; Zita Szalai 0000-0002-8722-0211; Bence Pál Barta 0000-0002-5309-8633; János Balázs 0000-0003-1775-6915; Zsolt Rázga 0000-0003-4717-8482; Edit Hermesz 0000-0002-0543-6693; Mária Bagyánszki 0000-0003-3533-9461.

Author contributions: Bódi N was responsible for the conceptualization, methodology, investigation, writing, funding acquisition; Mezei D, Barta BP, Chakraborty P were responsible for the investigation, formal analysis; Szalai Z was responsible for the visualization; Balázs J was responsible for the validation; Hermesz E was responsible for the validation, supervision; Rázga Z was responsible for the resources; Bagyánszki M was responsible for the visualization, writing-review and editing, supervision.

Supported by European Union and the Hungarian Government in the framework, No. EFOP-3.6.1-16-2016-00008; Hungarian NKFIH fund project, No. FK131789 (to Bó di N); János Bolyai Research Scholarship of the Hungarian

Nikolett Bódi, Diána Mezei, Zita Szalai, Bence Pál Barta, János Balázs, Mária Bagyánszki, Department of Physiology, Anatomy and Neuroscience, Faculty of Science and Informatics, University of Szeged, Szeged 6726, Hungary

Payal Chakraborty, Edit Hermesz, Department of Biochemistry and Molecular Biology, Faculty of Science and Informatics, University of Szeged, Szeged 6726, Hungary

Zsolt Rázga, Department of Pathology, Faculty of Medicine, University of Szeged, Szeged 6720, Hungary

Corresponding author: Mária Bagyánszki, PhD, Associate Professor, Department of Physiology, Anatomy and Neuroscience, Faculty of Science and Informatics, University of Szeged, Közép fasor 52, Szeged 6726, Hungary. bmarcsi@bio.u-szeged.hu

Abstract

BACKGROUND

The importance of the neuronal microenvironment has been recently highlighted in gut region-specific diabetic enteric neuropathy. Regionally distinct thickening of endothelial basement membrane (BM) of intestinal capillaries supplying the myenteric ganglia coincide with neuronal damage in different intestinal segments. Accelerated synthesis of matrix molecules and reduced degradation of matrix components may also contribute to the imbalance of extracellular matrix dynamics resulting in BM thickening. Among the matrix degrading proteinases, matrix metalloproteinase 9 (MMP9) and its tissue inhibitor (TIMP1) are essential in regulating extracellular matrix remodelling.

AIM

To evaluate the intestinal segment-specific effects of diabetes and insulin replacement on ganglionic BM thickness, MMP9 and TIMP1 expression.

METHODS

Ten weeks after the onset of hyperglycaemia gut segments were taken from the duodenum and ileum of streptozotocin-induced diabetic, insulin-treated diabetic and sex- and age-matched control rats. The thickness of BM surrounding myenteric ganglia was measured by electron microscopic morphometry. Whole-

Academy of Sciences (to Bódi N); and New National Excellence Program of the Ministry for Innovation and Technology from the source of the National Research, Development and Innovation Fund, No. ÚNKP-20-5 (to Bódi N).

Institutional review board statement: The study was reviewed and approved by Csaba Varga, the head of Dept. of Physiology, Anatomy and Neuroscience.

Institutional animal care and use committee statement: All animal experiments conformed to the internationally accepted principles for the care and use of laboratory animals.

Conflict-of-interest statement: I certify that there is no actual or potential conflict of interest in relation to this article.

Data sharing statement: Dataset available from the corresponding author at bmarcsi@bio.u-szeged.hu e-mail address.

ARRIVE guidelines statement: The authors have read the ARRIVE guidelines, and the manuscript was prepared and revised according to the ARRIVE guidelines.

Manuscript source: Invited manuscript

Specialty type: Gastroenterology and hepatology

mount preparations of myenteric plexus were prepared from the different gut regions for MMP9/TIMP1 double-labelling fluorescent immunohistochemistry. Post-embedding immunogold electron microscopy was applied on ultrathin sections to evaluate the MMP9 and TIMP1 expression in myenteric ganglia and their microenvironment from different gut segments and conditions. The MMP9 and TIMP1 messenger ribonucleic acid (mRNA) level was measured by quantitative polymerase chain reaction.

RESULTS

Ten weeks after the onset of hyperglycaemia, the ganglionic BM was significantly thickened in the diabetic ileum, while it remained intact in the duodenum. The immediate insulin treatment prevented the diabetes-related thickening of the BM surrounding the ileal myenteric ganglia. Quantification of particle density showed an increasing tendency for MMP9 and a decreasing tendency for TIMP1 from the proximal to the distal small intestine under control conditions. In the diabetic ileum, the number of MMP9-indicating gold particles decreased in myenteric ganglia, endothelial cells of capillaries and intestinal smooth muscle cells, however, it remained unchanged in all duodenal compartments. The MMP9/TIMP1 ratio was also decreased in ileal ganglia only. However, a marked segment-specific induction was revealed in MMP9 and TIMP1 at the mRNA levels.

CONCLUSION

These findings support that the regional decrease in MMP9 expression in myenteric ganglia and their microenvironment may contribute to extracellular matrix accumulation, resulting in a region-specific thickening of ganglionic BM.

Key Words: Type 1 diabetes; Diabetic enteric neuropathy; Neuronal microenvironment; Basement membrane; Matrix metalloproteinase 9; Tissue inhibitor of metalloproteinase 1

Core Tip: These findings demonstrate an intestinal segment-specific thickening of basement membrane (BM) surrounding myenteric ganglia. In diabetes, ganglionic BM is thickened in the ileum, but not in the duodenum. Insulin prevented the diabetes-related BM thickening. The matrix degrading matrix metalloproteinase 9 (MMP9) expression was decreased in myenteric ganglia and its environment in the diabetic ileum, however, it remained unchanged in the duodenum. Similarly, MMP9/Tissue inhibitor of metalloproteinase 1 (TIMP1) ratio decreased only in ileal myenteric ganglia. Intestinal segment-specific induction of MMP9 and TIMP1 messenger ribonucleic acid levels was revealed. Regionally decreased MMP9 expression in ganglia correlates well with segment-specific thickening of ganglionic BM and these coincide with region-dependent enteric neuronal damage.

Citation: Bódi N, Mezei D, Chakraborty P, Szalai Z, Barta BP, Balázs J, Rázga Z, Hermesz E, Bagyánszki M. Diabetes-related intestinal region-specific thickening of ganglionic basement membrane and regionally decreased matrix metalloproteinase 9 expression in myenteric ganglia. *World J Diabetes* 2021; 12(5): 658-672
URL: https://www.wjgnet.com/1948-9358/full/v12/i5/658.htm
DOI: https://dx.doi.org/10.4239/wjd.v12.i5.658

INTRODUCTION

In the last few years, there has been an increasing emphasis on the importance of the neural microenvironment in the diabetic damage of the enteric nervous system[1-3]. Moreover, the region-specific susceptibility of enteric neurons to diabetic neuropathy and their sensibility to immediate insulin treatment[4,5] serve as further motivation to thoroughly investigate the molecular neural milieu in different intestinal segments.

Country/Territory of origin: Hungary

Peer-review report's scientific quality classification

Grade A (Excellent): 0
Grade B (Very good): B
Grade C (Good): 0
Grade D (Fair): 0
Grade E (Poor): 0

Received: February 2, 2021
Peer-review started: February 2, 2021
First decision: February 27, 2021
Revised: March 10, 2021
Accepted: April 21, 2021
Article in press: April 21, 2021
Published online: May 15, 2021

P-Reviewer: Slomiany BL
S-Editor: Zhang L
L-Editor: A
P-Editor: Ma YJ

Since enteric ganglia are not vascularized, the capillaries in close vicinity have a critical role to supply them with oxygen and nutrients[6]. It is well established that among others, the thickened endothelial basement membrane (BM) is one of the earliest histological hallmarks of diabetic microangiopathy contributing to impaired permeability function in retina or renal glomeruli[7-11]. Consistent with this, we revealed a strictly intestinal region-dependent thickening and separation of capillary BM in type 1 diabetic rat model[12]. Structural and morphological findings (*e.g.*, opened endothelial tight junctions, enlarged caveolar compartments, impaired distribution of endogenous albumin) suggesting altered permeability of intestinal capillaries in the vicinity of myenteric ganglia were also revealed[12].

There may be several reasons for capillary BM thickening. On the one hand, the diabetes-related enhanced expression of the prevalent BM components leads to thickened BM. High glucose-induced overexpression of collagen IV, fibronectin, laminin, agrin and tenascin was observed in different models[10,13-16]. On the other hand, due to the long-lasting hyperglycaemic condition, the decreased degradation of these BM components may also result in a thickened BM, even under good glycaemic control. In rats with diabetic nephropathy, the decreased metalloproteinase activity promotes the accumulation of collagen IV in the matrix[17]. Others also observed an accelerated matrix accumulation in metalloproteinase knockout mice[18]. Overall, the accumulation of extracellular matrix (ECM) molecules and/or the decreased degradation of matrix components may contribute to the imbalance in ECM dynamics and lead to BM thickening.

ECM proteins are degraded by several proteinases[19]. Among them, metalloproteinases are the most essential in regulating ECM remodelling[19]. Matrix metalloproteinases (MMPs) are calcium-dependent zinc-containing endopeptidases[20]. The MMP family has more than 20 members in vertebrates, most of them with basic three-domain structures and different ECM and other targets[21]. However, MMPs have not only proteinase activity, but are also implicated in other essential functions, like releasing apoptotic ligands, cytokine inactivation, cell proliferation and differentiation, angiogenesis, and host defense[19,21-23].

MMP9 is secreted by a wide variety of cells, such as macrophages, smooth muscle cells, endothelial cells, and it is one of the most extensively studied enzymes involved in ECM breakdown and turnover. Due to the crosstalk between ECM and inflammatory processes, MMPs are associated with the development of diabetic microvascular complications in different organs[24]. MMP activation accelerates apoptotic processes in retina[25]. There is correlation also between upregulated MMP expression and the progression of diabetic nephropathy[26,27]. Under diabetic conditions, MMP expression is influenced by high glucose level and reactive oxygen species[27]. Moreover, the endogenous tissue inhibitors of metalloproteinases (TIMPs), are crucial to determine the optimal proteolytic activity of MMPs[28]. Among the four members of TIMP family, TIMP1 has the strongest efficiency to inhibit most of the MMPs[29]. TIMPs can directly restrict MMP-dependent matrix proteolysis or indirectly facilitate ECM accumu-lation[29].

All enteric ganglia are surrounded with a continuous BM[6,30], and the components of this ECM sheet are not detectable inside the enteric ganglia[31]. Several studies dealt with the composition and alterations of ECM in the intestinal wall due to its impact on enteric ganglion formation during development[32-34]. The appropriate matrix composi-tion is indispensable for the development of enteric ganglia and normal nerve fibre function[33,35]. The relevance of different BM abnormalities was investigated in Hirschprung's disease[36-38], however, little is known about its role in other pathological processes, like diabetes-related enteric neuropathy.

We assume that structural and molecular alterations involved in maintaining the dynamic structure of ECM in the intestinal wall may contribute to the gut region-dependent diabetic neuropathy. Therefore, the primary goal of this study was to evaluate the effects of type 1 diabetes and immediate insulin replacement on BM thickness surrounding myenteric ganglia in different gut segments. Furthermore, we aimed to investigate the intestinal region-dependent expression of MMP9 and TIMP1 in myenteric ganglia and their microenvironment in control, diabetic and insulin-treated diabetic rats.

MATERIALS AND METHODS

Animal model

Adult male Wistar rats (Crl: WI BR; Toxi-Coop Zrt.) kept on standard laboratory chow

(Farmer-Mix Kft., Hungary) and with free access to drinking water, were used throughout the experiments. The rats, weighing 200-300 g, were divided randomly into three groups: streptozotocin (STZ)-induced diabetics (n = 4), STZ-induced diabetics with insulin treatment (n = 4) and sex- and age-matched controls (n = 4). The controls were treated with vehicle, while hyperglycaemia was induced by a single intraperitoneal injection of STZ (Sigma-Aldrich, Hungary) at 60 mg/kg as described previously[4,12]. The animals were considered diabetic if the non-fasting blood glucose concentration was higher than 18 mmol/L. From this time on, the insulin-treated hyperglycaemic group received a subcutaneous injection of insulin (Humulin M3; Eli Lilly Nederland, Netherlands) each morning (2 IU) and afternoon (2 IU). Equivalent volumes of saline were given subcutaneously to the rats in the diabetic and the control group. The blood glucose level and weight of each animal were measured weekly during the 10-wk experimental period. Those STZ-induced diabetic animals which recover spontaneously or their blood glucose level decreased under 18 mmol/L during the 10-wk experimental period did not participate in this study.

The animal protocol was designed to minimize pain or discomfort to the animals. The animals were acclimatized to laboratory conditions (23 °C, 12 h/12 h light/dark, 50% humidity, ad libitum access to food and water) for 2 wk prior to experimentation.

In all procedures involving experimental animals, the principles of the National Institutes of Health (Bethesda, MD, United States) guidelines and the EU directive 2010/63/EU for the protection of animals used for scientific purposes were strictly followed, and all the experiments were approved by the National Scientific Ethical Committee on Animal Experimentation (National Competent Authority), with the license number XX./1636/2019.

Tissue handling

Ten weeks after the onset of hyperglycaemia, the animals were euthanized by barbiturate overdose (150 mg/kg pentobarbital sodium i.v. injection) for tissue collection. The gut segments of the control, STZ-induced diabetic, and insulin-treated diabetic rats were dissected and rinsed in 0.05 mol/L phosphate buffer (PB; pH 7.4). Samples were taken from the duodenum (1 cm distal to the pylorus) and the ileum (1 cm proximal to the ileo–caecal junction), and processed for fluorescent immunohistochemistry, quantitative electron microscopy and quantitative polimerase chain reaction (qPCR). For double-labelling fluorescent immunohistochemistry, samples (2-3 mm) from different gut segments were fixed in 4% paraformaldehyde (PFA) and embedded in melted paraffin. For electron microscopic studies, small pieces (2-3 mm) of the gut segments were fixed in 2% PFA and 2% glutaraldehyde solution and then further fixed for 1 h in 1% OsO_4. After rinsing in buffer and dehydrating in increasing ethanol concentrations and acetone, they were embedded in Embed812 (Electron Microscopy Sciences, United States). The Embed blocks were used to prepare ultrathin (70 nm) sections, which were mounted on nickel grids and processed for morphometrical study and immunogold labelling. For qPCR study, the 3-cm-long gut segments were cut along the mesentery and pinched flat. The layer of mucosa and submucosa was removed, and the residual material (myenteric plexus and intestinal smooth muscle layers) was snap-frozen in liquid nitrogen and stored at -80 °C until use.

Double-labelling fluorescent immunohistochemistry

For double-labelling immunohistochemistry, paraffin-sections (3.5 μm) derived from different gut segments were immunostained with MMP9 and TIMP1. Briefly, after blocking in TRIS-buffered saline (TBS) containing 1% bovine serum albumin and 10% normal goat serum, the sections were incubated overnight with anti-MMP9 (mouse monoclonal immunoglobulin G (IgG); Abcam, UK; final dilution 1:100) and anti-TIMP1 (rabbit polyclonal IgG; Santa Cruz Biotechnology, United States; final dilution 1:50) primary antibodies at 4 °C. After washing in TBS with 0.025% Triton X-100, sections were incubated with anti-mouse Cy™3 (Jackson ImmunoResearch Laboratories, Inc., United States; final dilution 1:200) and anti-rabbit Alexa Fluor 488 (Life Technologies Corporation, Molecular Probes, Inc., United States; final dilution 1:200) secondary antibodies for 1 h at room temperature. Negative controls were performed by omitting the primary antibody when no immunoreactivity was observed. Sections were mounted on slides in Fluoromount™ Aqueous Mounting Medium (Sigma-Aldrich, Hungary), observed and photographed with a Zeiss Imager Z.2 fluorescent microscope equipped with an Axiocam 506 mono camera.

Transmission electron microscopy

Morphometric study: For ultrathin sectioning, four Embed blocks were used for each intestinal segment and each condition (control, STZ-induced diabetics, and insulin-treated diabetics). Three grids per block were counterstained with uranyl acetate (Merck, Germany) and lead citrate (Merck, Germany) and were examined and photographed with a JEOL JEM 1400 transmission electron microscope. Montage photographs of twelve myenteric ganglia per intestinal segment per condition were made at a magnification of 20000 × and the thickness of the BM were measured at random points around the ganglia with the help of a limited size (700 nm × 700 nm) grid net. The mean thickness was then calculated for each ganglion by using the AnalySIS 3.2 program (Soft Imaging System GmbH, Germany).

Post-embedding immunohistochemistry

The Embed blocks used previously for the electron microscopic morphometry also served for the MMP9 and TIMP1 post-embedding immunohistochemistry. Ultrathin sections from each block were sequentially incubated overnight in anti-MMP9 mouse monoclonal IgG (Abcam, United Kingdom; final dilution 1:50) or anti-TIMP1 rabbit polyclonal IgG (Santa Cruz Biotechnology, United States; final dilution 1:50) primary antibodies, followed by colloidal gold conjugated anti-mouse IgG (conjugated to 18 nm colloidal gold; Jackson Immunoresearch, United States; final dilution 1:20) or anti-rabbit IgG (conjugated to 18 nm colloidal gold; Jackson Immunoresearch, United States; final dilution 1:20) secondary antibodies for 3 h, with extensive TBS washing in-between. The specificity of the immunoreaction was assessed in all cases by omitting the primary antibodies in the labelling protocol and incubating the sections only in the gold conjugated secondary antibodies. Sections were counterstained with uranyl acetate (Merck, Germany) and lead citrate (Merck, Germany) and were examined and photographed with a JEOL JEM 1400 transmission electron microscope. The quantitative properties of gold particles coding for MMP9 or TIMP1 were determined in the myenteric ganglia, the endothelium of capillaries in the vicinity of these ganglia and the intestinal smooth muscle cells. Counting was performed on digital photographs at a magnification of 20000 × with the AnalySIS 3.2 program (Soft Imaging System GmbH, Germany). Montage pictures of twelve ganglia, the entire endothelial profile of eleven well-oriented capillaries and eleven field of view of the surrounding smooth muscle cells per intestinal segment per condition were used. The intensity of the labelling was expressed as the total number of gold particles per unit area.

RNA preparation, reverse transcription and qPCR

Intestinal tissue samples were homogenized in RNA Bee reagent (Tel-Test Inc., United States) and total RNA was prepared according to the procedure suggested by the manufacturer. For assessing RNA concentration and purity, the absorbance of RNA samples was measured at 260 and 280 nm using NanoDrop 1000 UV/VIS Spectrophotometer (Thermo Scientific, United States). The RNA concentration was calculated using the A260 = 1.0 equivalent to approximately 40 g/mL single-stranded RNA equation. The A260/A280 ratio approximately 1.9 was accepted for clean RNA. First-strand cDNA was synthesized by using 2.5 μg total RNA as template, 200 pmol of each dNTP (Thermo Scientific, United States), 200 U Maxima H Minus Reverse Transcriptase (Thermo Scientific, United States) and 500 pmol random hexamer primers (Sigma-Aldrich, Hungary) in a final volume of 20 μL, and incubated for 10 min at 37 °C, followed by 45 min at 52 °C. Real-time qPCR was performed for gene expression studies, using Luminaris Color HiGreen Low ROX qPCR Master Mix (Thermo Scientific, United States) in Applied Biosystems 7500 Real-Time PCR System (Life Technologies, Hungary). The qPCR reactions were carried out with a temperature program of 10 min at 95 °C (initial denaturing), followed by 45 cycles of 15 s at 95 °C; 30 s at the annealing temperature 63 °C followed by a melting curve stage with temperature ramping from 60 to 95 °C and a final cooling for 30 s at 40 °C. The quantities of examined messenger ribonucleic acid (mRNAs) were normalized to that of 18 S ribosomal RNA, and gene expression was calculated in terms of $2^{\Delta\Delta Ct}$ method[39].

Primers

Primers were designed based on the data bank entries. For normalization of the amounts of MMP9 and TIMP1 mRNA, the 18 S RNA level was used as internal standard. MMP9 2F: 5′ CTCTACACGGAGCACGGCAACG 3′; MMP9 2R: 5′ CGGTGGTGGCGCACCAGCG 3′.TIMP1 2F: 5′ ACAGGTTTCCGGTTCGCCTAC 3′;

TIMP1 2R: 5′ CTGCAGGCAGTGATGTGCAA 3′. 18S F: 5′ GAAACGGCTACC ACATCCAAGG 3′; 18S R: 5′ CCGCTCCCAAGATCCAACTACG 3′.

Statistical analysis

Statistical analysis was performed with Kruskal-Wallis test, and Dunn's multiple comparisons test (electron microscopic study), or one-way analysis of variance with Newman-Keuls test (Table 1 and qPCR study). Statistical analysis of RT-qPCR reactions for each animal were performed in triplicate to increase the reliability of the measurements. All analyses were carried out with GraphPad Prism (GraphPad Software, United States). A probability of $P < 0.05$ was set as the level of significance.

RESULTS

Disease characteristics of diabetic and insulin-treated diabetic rats

The general characteristics of the STZ-induced diabetic and insulin-treated diabetic, as well as the control animals are shown in Table 1. Untreated diabetic rats were characterized by a significantly reduced body weight and a markedly increased blood glucose concentration (26.23 ± 1.89 mmol/L) as compared to the sex-and age-matched controls (5.99 ± 0.19 mmol/L). In the immediate insulin replacement group, the body weight of the animals was similar to controls by the end of the experiment. The blood glucose concentration of insulin-treated rats (7.13 ± 1.37 mmol/L) remained at the control level during the 10 wk experimental period.

Morphometry of the BM surrounding myenteric ganglia

Myenteric ganglia are surrounded by a thin BM, which delimits the ganglia from the adjacent tissues. The collagen fibrils located in the extracellular space never enter into the ganglia (Figure 1A).

In controls, BM thickness was the same in the proximal and distal part of the small intestine (approximately 34-36 nm), however, a region-specific thickening was revealed in diabetic rats. The ganglionic BM was significantly thicker in the diabetic ileum relative to control values (44.04 ± 1.62 nm *vs* 34.85 ± 1.11 nm, $P < 0.0001$), whereas in the duodenum it did not exceed that of the controls (Figure 1B). Although the diabetes-related BM thickening was prevented by immediate insulin treatment in the ileum, the BM was significantly thinner (26.98 ± 0.93 nm) in this region in insulin-treated rats (Figure 1B).

Presence of MMP9 and TIMP1 immunoreactivity in the gut wall

Double-labelling fluorescent microscopy revealed MMP9 and TIMP1 immunoreactivity in myenteric ganglia and their environment (Figure 2). The intensity of the fluorescent labelling varied among different structures of the gut wall: it was the lowest in the ganglia, higher in the intestinal blood vessels, and pronouncedly intense in the circular and longitudinal smooth muscle layers (Figure 2).

Quantitative changes in MMP9 expression in different cellular compartments

The expression of MMP9 was further demonstrated by gold-labelling immunoelectron microscopy in myenteric ganglia, endothelial cells of capillaries in the vicinity of these ganglia and smooth muscle cells (Figure 3). The 18 nm gold particles indicating MMP9 were often detected in cytosol, nuclei, intracellular organelles of the neuronal perikaryon (Figure 3A) and neuropil region (Figure 3B) of the ganglia, caveolar compartments, and plasma membrane of endothelial and smooth muscle cells (Figure 3C).

In control animals, the density of MMP9-labeling gold particles was significantly higher in the myenteric ganglia of the ileum than in the duodenal segment ($P < 0.001$; Figure 4A). Also, higher ileal density of MMP9 particles was observed in endothelial and smooth muscle cells (data not shown separately, but visible on Figure 5B and C).

In diabetic rats, the number of MMP9-labeling gold particles significantly decreased in the myenteric ganglia (Figure 5A), capillary endothelium (Figure 5B) and intestinal smooth muscle (Figure 5C) of the ileum. The greatest decrease has been observed in the endothelial cells of diabetics, where the number of MMP9 particles was more than half of the controls (0.75 ± 0.11 *vs* 1.66 ± 0.26). The immediate insulin treatment only partially prevented the diabetes-related alterations in MMP9 expression. However, in the diabetic duodenum, the number of MMP9 gold particles did not change in the myenteric ganglia or in the other cell types in either of the experimental groups

Table 1 Weight and glycaemic characteristics of the experimental groups

	Weight (g)		Blood glucose level (mmol/L)	
	Initial	Final	Initial	Final (average)
Controls (n = 4)	266 ± 18.85	460.25 ± 22.34[b]	6.48 ± 0.2	5.99 ± 0.19
Diabetics (n = 4)	274 ± 17.11	382.5 ± 17.69[a,c]	6.4 ± 0.24	26.23 ± 1.89[b,d]
Insulin-treated diabetics (n = 4)	274 ± 15.36	457.25 ± 29.33[b,e]	6.28 ± 0.09	7.13 ± 1.37[f]

[a]P < 0.01.
[b]P < 0.0001 *vs* initial.
[c]P < 0.05.
[d]P < 0.0001 *vs* final controls.
[e]P < 0.05.
[f]P < 0.0001 *vs* final diabetics. Data are expressed as mean ± SEM.

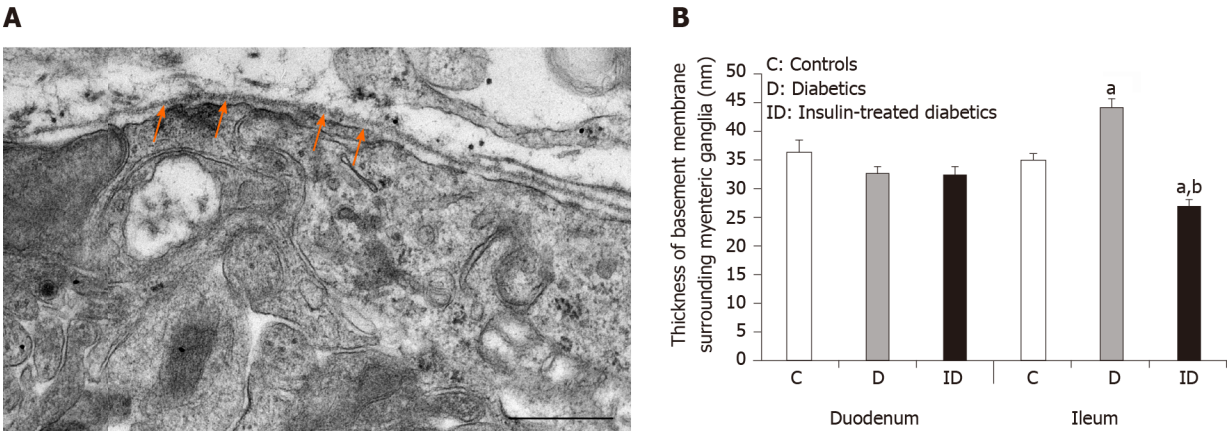

Figure 1 Representative electron micrograph of a myenteric ganglion from an insulin-treated diabetic rat. A: The myenteric ganglion is surrounded by basement membrane (BM) (arrows). Scale bar: 500 nm; B: Quantitative evaluation of BM thickness in different gut segments of control, diabetic, and insulin-treated diabetic rats. The thickening of BM surrounding myenteric ganglia remained unchanged in the duodenum, however it increased significantly in the ileum of diabetic rats. Immediate insulin treatment prevented BM thickening in the ileum. [a]P < 0.0001 (relative to the controls); [b]P < 0.0001 (between diabetics and insulin-treated diabetics).

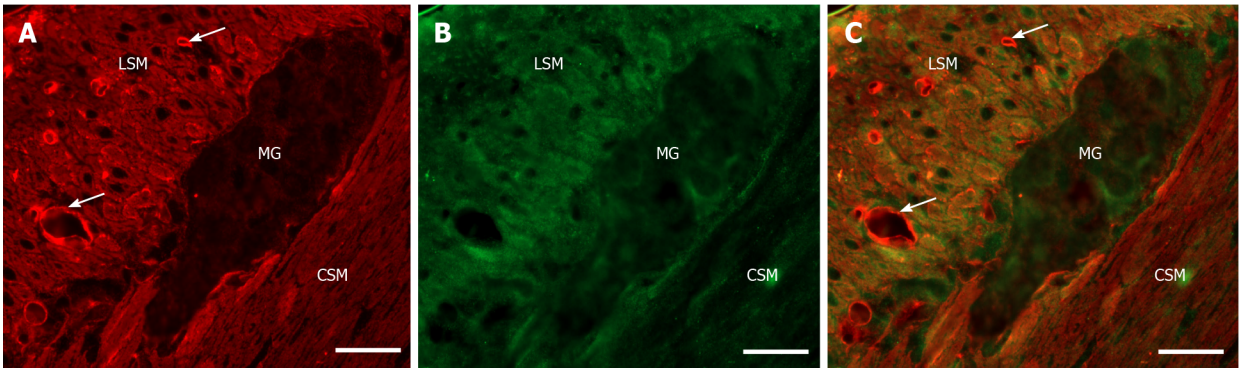

Figure 2 Representative fluorescent micrograph of a paraffin section of myenteric ganglia from the ileum of a control rat after matrix metalloproteinase 9-tissue inhibitor of metalloproteinase 1 double-labelling immunohistochemistry. A: Matrix metalloproteinase 9 immunoreactivity is indicated in red; B: tissue inhibitor of metalloproteinase 1 immunoreactivity is shown in green; and C: The merge is depicted on. Scale bar: 20 μm. MG: Myenteric ganglia; LSM: Longitudinal smooth muscle layer; CSM: Circular smooth muscle layer; arrows-blood vessels.

(Figure 5).

Quantitative changes in TIMP1 expression and MMP9/TIMP1 ratio

TIMP1 displayed a quite low, but region-dependent expression in the myenteric

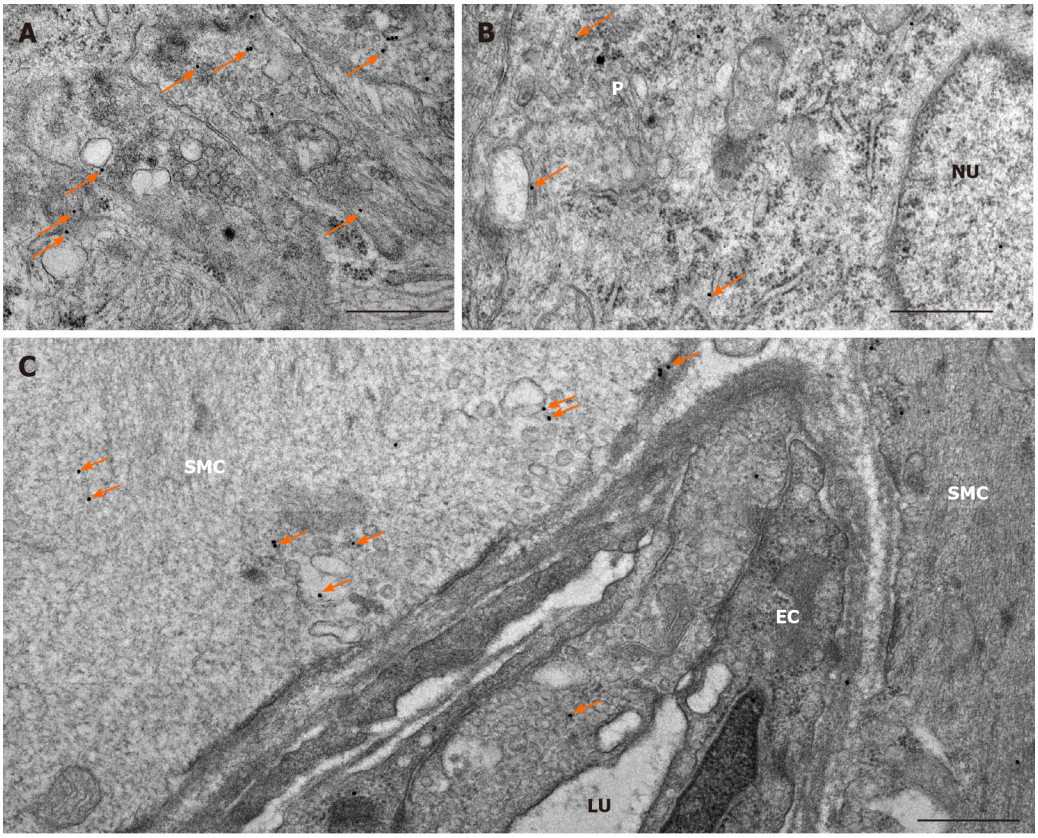

Figure 3 Representative electron micrographs subjected to matrix metalloproteinase 9 post-embedding immunohistochemistry. A: Myenteric ganglia from a control duodenum; B: A diabetic ileum; and C: Capillary endothelium and intestinal smooth muscle from a control duodenum. The 18 nm gold particles (arrows) indicating matrix metalloproteinase 9 were observed in cytosol, nuclei or in association with intracellular organelles and plasma membrane. Scale bars: 500 nm. P: Neuronal perikaryon; N: Nucleus; SMC: Smooth muscle cell; EC: Endothelial cell; LU: Capillary lumen.

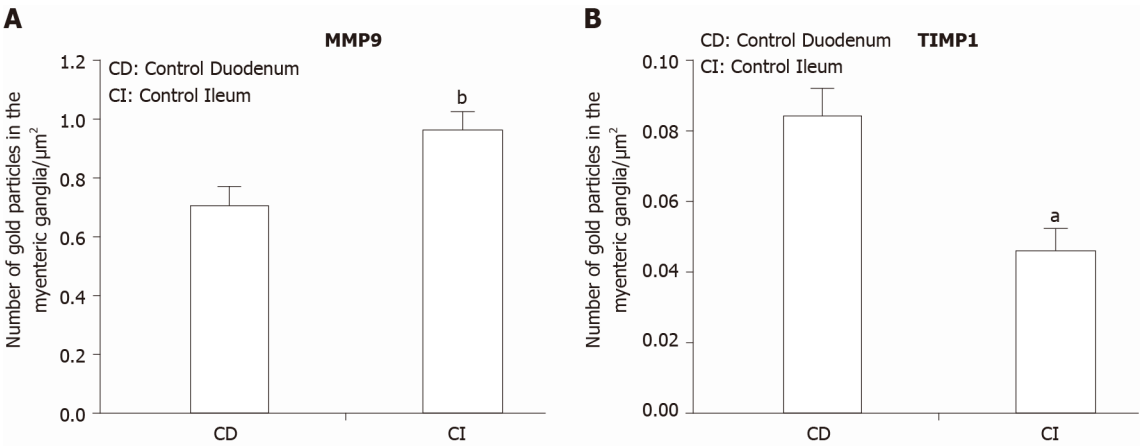

Figure 4 Quantitative changes in MMP9 and TIMP1 expression. A: Quantitative evaluation of matrix metalloproteinase 9 (MMP9); and B: Quantitative evaluation of tissue inhibitor of metalloproteinase 1 (TIMP1) labelling gold particles in myenteric ganglia from different gut segments of control rats. In control conditions, the number of MMP9 particles was significantly higher, while TIMP1-labeling was significantly lower in the distal part of the small intestine. Data are expressed as means ± SEM. $^{a}P < 0.01$ and $^{b}P < 0.001$ (between control duodenum and control ileum).

ganglia of different gut segments in control conditions. The number of TIMP1-labeling gold particles was half in the ileal than in the duodenal ganglia ($P < 0.01$; Figure 4B). There were no significant differences in the distribution of TIMP1 gold particles between different intestinal regions in other control cell types (data not shown). In addition, neither the hyperglycaemia nor the immediate insulin treatment resulted in any significant alterations in the number of TIMP1-labeling gold particles in either of the cellular compartments (data not shown).

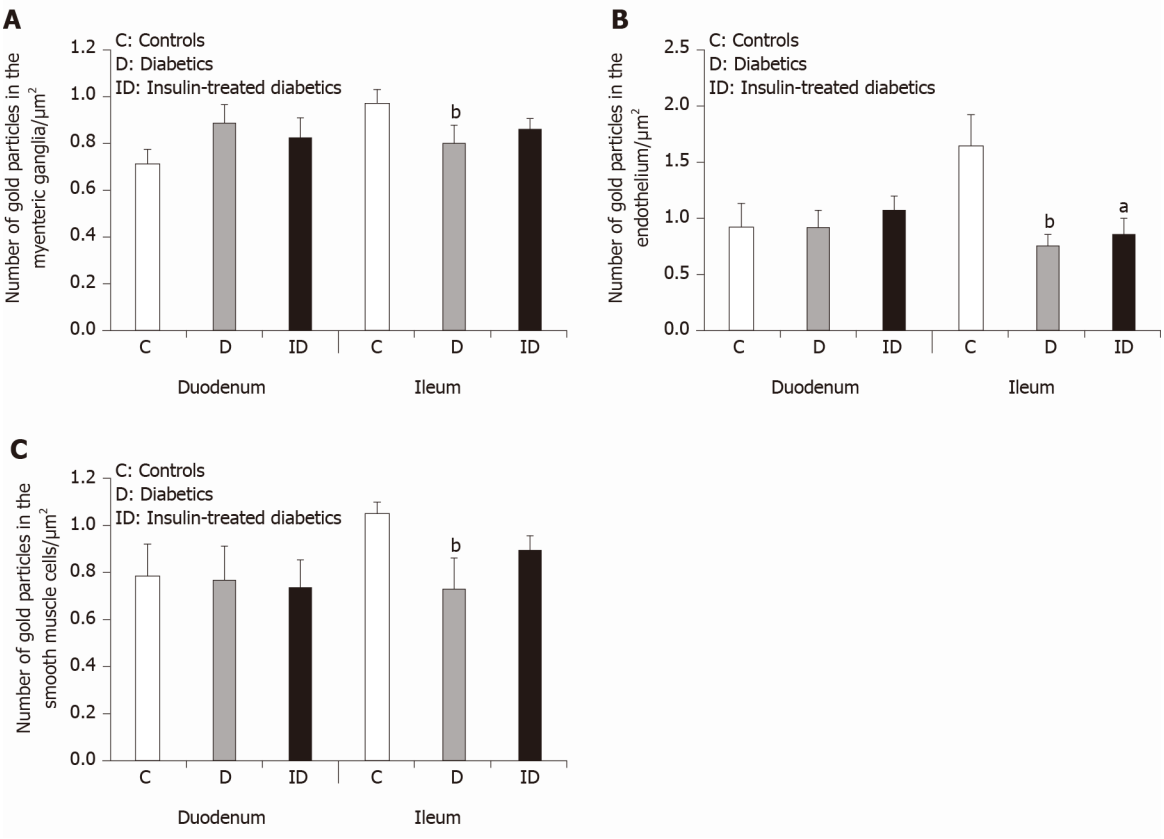

Figure 5 Quantitative changes in matrix metalloproteinase 9 expression in different cellular compartments. A: Quantitative evaluation of matrix metalloproteinase 9 (MMP9)-labeling gold particles in myenteric ganglia; B: Capillary endothelium; and C: Intestinal smooth muscle cells from different gut segments of control, diabetic, and insulin-treated diabetic rats. In diabetics, the number of MMP9-labeling gold particles was significantly decreased in all cellular compartments of the ileum, while it was unchanged in the duodenum relative to controls. The number of gold particles was closer to the control values after immediate insulin treatment. Data are expressed as means ± SEM. $^{a}P < 0.05$ and $^{b}P < 0.01$ (relative to controls).

However, a region-specific MMP9/TIMP1 ratio was observed in the myenteric ganglia. While the MMP9/TIMP1 ratio remained unchanged in the duodenum, the decrease in the ratio was nearly 50% in the ileal ganglia of diabetic rats (Figure 6). The MMP9/TIMP1 ratio was more than double in the duodenum, while it was close to the control value in the ileum in the insulin-treated group (Figure 6).

Quantitative alterations in mmp9 and timp1 mRNA expression

The expression level of MMP9 mRNA markedly increased in both gut segments under chronic hyperglycaemic conditions. The rate of induction was approximately 5.5-fold in tissue homogenates prepared from the diabetic duodenum, and approximately 7.0-fold in the diabetic ileum relative to controls and normalized to the endogenous 18S RNA as reference (Figure 7).

In parallel, TIMP1 mRNA expression was highly upregulated (approximately 5-fold) in tissue homogenates originating from the ileum, while it remained unchanged in duodenal homogenates of diabetic rats (Figure 7).

DISCUSSION

In accordance with our principle findings that diabetic myenteric neuropathy is intestinal region-dependent[4], and that the neuronal microenvironment is also suffering from a series of strictly region-specific diabetic damages[12,40], the present study provides more evidence of gut segment-specific, diabetes-related alterations of the ECM biology in myenteric ganglia, intestinal capillaries and smooth muscle of the gut wall.

We have shown for the first time that the BM surrounding myenteric ganglia is regionally thickened along the small intestine. The thickness was increased by more than 25% in the ileum, while it was unchanged in the duodenum of diabetic rats.

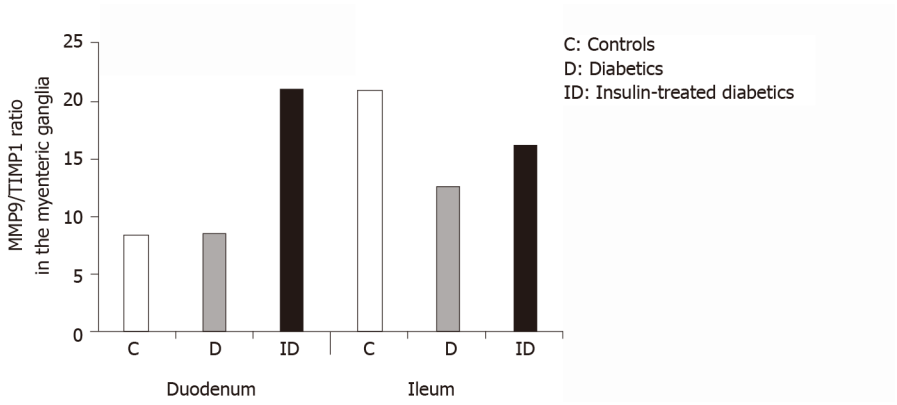

Figure 6 The ratio of matrix metalloproteinase 9 and tissue inhibitor-labeling gold particles in myenteric ganglia of different gut segments of control, diabetic, and insulin-treated diabetic rats. In diabetic rats, the matrix metalloproteinase 9/tissue inhibitor of metalloproteinase 1 ratio was not altered in duodenal, but was markedly decreased in ileal ganglia. The immediate insulin replacement did not restore the equilibrium ratio observed in controls.

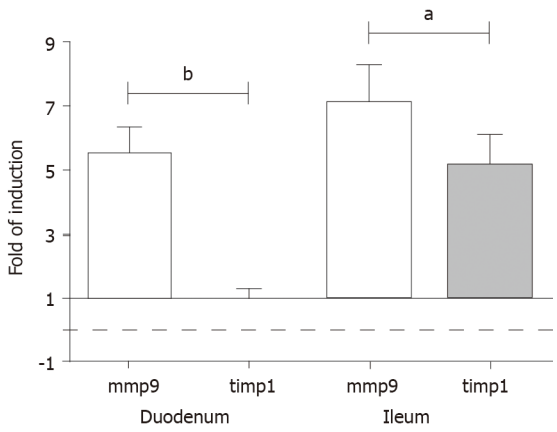

Figure 7 Fold change in the messenger ribonucleic acid levels of matrix metalloproteinase 9 and tissue inhibitor of metalloproteinase 1 genes, measured by real-time fluorescence-based quantitative polymerase chain reaction using the $2^{\Delta\Delta Ct}$ method. Data sets are presented as the fold change in gene expression normalized to the endogenous reference (RNA18S) and relative to the untreated controls. Data are expressed as means ± standard deviation. $^{a}P < 0.001$ and $^{b}P < 0.0001$.

Using the same type 1 diabetic rat model, we formerly demonstrated that the endothelial BM of intestinal capillaries supplying the enteric ganglia displayed similar structural alterations[12]. The thickening and separation of capillary BM was pronounced in the distal part of the gastrointestinal tract, but not in the duodenum of diabetics[12], which suggests optimal and very stable conditions in the duodenum while a more susceptible microenvironment is plausible in the ileum along the proximal-distal axis of the gut. Other findings include increased amount of ECM proteins (laminin-1 and fibronectin), as well as BM thickening of the small intestinal smooth muscle cells in diabetic rats[41], and also significant thickening of perineurial cell BM and loss of myelinated nerve fibres in diabetic peripheral neuropathies[42-44]. The immediate insulin replacement prevented diabetes-related BM thickening surrounding the ileal myenteric ganglia, as it inhibited the BM thickening of capillary endothelium[12] or reversed the hyperglycaemia-induced ECM accumulation in the intestinal smooth muscle layers[41]. Among the underlying mechanisms of ECM accumulation resulting in both ganglionic and endothelial BM thickening, the matrix degrading metalloproteinases have become the focus of the present study. We have shown that MMP9 and TIMP1 is present in myenteric ganglia and their environment using fluorescent and electron microscopy. The ultrastructural localization of these markers within the cytoplasm and nuclei of the enteric neurons, endothelial and smooth muscle cells was in agreement with other findings[45,46]. The nuclear localization of MMPs may have a role in regulation the activity of DNA-repairing and apoptotic proteins[47,48].

Quantitative immunogold labelling showed that the MMP9 particle density increased, while the TIMP1 particle density decreased in myenteric ganglia along the proximal-distal axis of the small intestine under control conditions. In addition to this opposite tendency, we observed that the particle density of TIMP1 was an order of magnitude lower than that of MMP9. In diabetic rats, the MMP9-indicating gold particles decreased in all cell types of the ileum, however, they remained unchanged in all duodenal compartments. Moreover, the MMP9/TIMP1 ratio was also decreased only in the ileal ganglia, but not in the duodenum. Immediate insulin replacement prevented diabetic alterations only in part as it was described in other studies[4,5,12].

The region-dependent BM thickening and changes in MMP production in different cellular compartments correlate well with each other. In the diabetic ileum, the decrease in MMP9 expression both in myenteric ganglia, and endothelial and smooth muscle cells suggests a decreased breakdown of ECM components resulting in ECM accumulation and thickening of BM around the myenteric ganglia and also the intestinal capillaries[12]. However, in the diabetic duodenum, where MMP9 production remained optimal in all cell types, the thickness of ganglionic and endothelial BM also remained unchanged[12].

Although we did not observe significant changes in the distribution of TIMP1 protein-detecting gold particles in different cell types under diabetic conditions and after insulin treatment, the segment-specific induction of both MMP9 and TIMP1 mRNA expression was demonstrated. Meanwhile, the MMP9 induction was not accompanied by altered TIMP1 expression in the duodenal tissue homogenates of diabetics, however, in the ileal samples, a 7-fold increase in MMP9 mRNA level was detected, along with a great upregulation in TIMP1 mRNA expression. The regulation of MMPs/TIMPs expression and activity is complex, involving both transcriptional and post-transcriptional mechanisms using multiple signal pathways, microRNA modulation, post-translational modifications and extracellular inhibition[21,49-51]. Based on these findings, we presume that despite of the MMP9 transcriptional alterations, due to post-transcriptional modifications[49], the balance in the production of MMP9 and TIMP1 proteins was retained in the duodenum, which contributes to the maintenance of optimal ECM dynamics in this segment. In contrast, in the ileum, not only MMP9 but also TIMP1 transcription was highly upregulated, resulting in MMP9 protein underproduction and ECM accumulation. Inconsistent alterations of MMP9 mRNA and protein expression presuming post-transcriptional regulation were also observed in diabetic nephropathy[52]. Moreover, upregulated microRNA production resulted in decreased MMP9 expression, which in turn contributed to renal fibrosis in diabetic kidney[52,53]. Decreased matrix degradation due to increased MMP mRNA level, but decreased activity was also documented in diabetic nephropathy[17,54], modulated by advanced glycation end products[55]. Increased fibrosis was also demonstrated in MMP knockout mice[18]. In contrast, some studies report that MMP overexpression promotes renal fibrosis due to a possible interplay with TIMPs[51,56], while others revealed that MMP2 and MMP9 triggered mitochondrial damage and apoptotic processes in retinal capillaries[57-59].

However, it certainly seems that the imbalance in MMP/TIMP ratio[60,61] caused by various molecular mechanisms disturbs the equilibrium of ECM degradation and turnover and contributes to several inflammatory processes, as well as vascular or neuronal damage, which requires further investigations.

CONCLUSION

Overall, in the present study, we provided evidence that the region-dependent thickening of ganglionic basement membrane is closely related to the regionally decreased MMP9 expression in myenteric ganglia and its environment, coinciding with the intestinal region-specific enteric neuropathy in type 1 diabetes.

ARTICLE HIGHLIGHTS

Research background

The diabetic damage of enteric neurons and intestinal capillaries supplying the enteric ganglia are strictly intestinal region dependent. Therefore, the underlying molecular differences in the neuronal environment should be more emphasized.

Research motivation
To prove the presence of essential regional differences in the neuronal milieu which may explain the gut segment-specific enteric neuropathy and vascular dysfunction.

Research objectives
To reveal the impact of diabetes and immediate insulin treatment on the thickness of basement membrane (BM) surrounding myenteric ganglia, as well as the expression of matrix metalloproteinase 9 (MMP9) and its tissue inhibitor of metalloproteinase 1 (TIMP1) which are key players in regulating extracellular matrix dynamics.

Research methods
Electron microscopic morphometry, fluorescent and gold-labelling immunohistochemistry and quantitative polymerase chain reaction were applied to study the myenteric ganglia and their environment in the different gut segments of diabetic, insulin-treated diabetic and control rats.

Research results
In the diabetic ileum, the ganglionic BM was significantly thickened which was prevented by insulin treatment. These changes were also reflected in a decrease in MMP9/TIMP1 ratio in ileal myenteric ganglia. However, in the duodenum of diabetics neither the ganglionic BM thickness nor the MMP9/TIMP1 ratio were changed.

Research conclusions
Regionally decreased MMP9 expression in ganglia and region-dependent ganglionic BM thickening correlate well with intestinal segment-specific enteric neuropathy.

Research perspectives
Based on these findings in type 1 diabetic rat model, we are planning to expand our investigations to type 2 diabetes in the future.

ACKNOWLEDGEMENTS
We thank Erika Németh and Katalin Arany for the excellent technical assistance.

REFERENCES
1 **Bagyánszki M**, Bódi N. Diabetes-related alterations in the enteric nervous system and its microenvironment. *World J Diabetes* 2012; **3**: 80-93 [PMID: 22645637 DOI: 10.4239/wjd.v3.i5.80]
2 **Bodi N**, Bagyanszki M. Diabetic enteric neuropathy: imbalance between oxidative and antioxidative mechanisms. In: Preedy VR, editor. Diabetes: Oxidative Stress and Dietary Antioxidants. Academic Press 2020: 25-33 [DOI: 10.1016/B978-0-12-815776-3.00003-6]
3 **Niesler B**, Kuerten S, Demir IE, Schäfer KH. Disorders of the enteric nervous system - a holistic view. *Nat Rev Gastroenterol Hepatol* 2021 [PMID: 33514916 DOI: 10.1038/s41575-020-00385-2]
4 **Izbéki F**, Wittman T, Rosztóczy A, Linke N, Bódi N, Fekete E, Bagyánszki M. Immediate insulin treatment prevents gut motility alterations and loss of nitrergic neurons in the ileum and colon of rats with streptozotocin-induced diabetes. *Diabetes Res Clin Pract* 2008; **80**: 192-198 [PMID: 18242757 DOI: 10.1016/j.diabres.2007.12.013]
5 **Bódi N**, Szalai Z, Chandrakumar L, Bagyánszki M. Region-dependent effects of diabetes and insulin-replacement on neuronal nitric oxide synthase- and heme oxygenase-immunoreactive submucous neurons. *World J Gastroenterol* 2017; **23**: 7359-7368 [PMID: 29151690 DOI: 10.3748/wjg.v23.i41.7359]
6 **Gabella G**. On the ultrastructure of the enteric nerve ganglia. *Scand J Gastroenterol Suppl* 1982; **71**: 15-25 [PMID: 6951271]
7 **Roy S**, Sato T, Paryani G, Kao R. Downregulation of fibronectin overexpression reduces basement membrane thickening and vascular lesions in retinas of galactose-fed rats. *Diabetes* 2003; **52**: 1229-1234 [PMID: 12716757 DOI: 10.2337/diabetes.52.5.1229]
8 **Fioretto P**, Mauer M. Histopathology of diabetic nephropathy. *Semin Nephrol* 2007; **27**: 195-207 [PMID: 17418688 DOI: 10.1016/j.semnephrol.2007.01.012]
9 **Lee SE**, Ma W, Rattigan EM, Aleshin A, Chen L, Johnson LL, D'Agati VD, Schmidt AM, Barile GR. Ultrastructural features of retinal capillary basement membrane thickening in diabetic swine. *Ultrastruct Pathol* 2010; **34**: 35-41 [PMID: 20070152 DOI: 10.3109/01913120903308583]
10 **Chronopoulos A**, Trudeau K, Roy S, Huang H, Vinores SA. High glucose-induced altered basement membrane composition and structure increases trans-endothelial permeability: implications for

diabetic retinopathy. *Curr Eye Res* 2011; **36**: 747-753 [PMID: 21780924 DOI: 10.3109/02713683.2011.585735]
11 **Yamakawa T**, Kawaguchi T, Kitamura H, Kadomura M, Nishimura M, Yokoo T, Imasawa T. Glomerular basement membrane duplication is a predictor of the prognosis of diabetic nephropathy in patients with type 2 diabetes. *Clin Exp Nephrol* 2019; **23**: 521-529 [PMID: 30467801 DOI: 10.1007/s10157-018-1674-z]
12 **Bódi N**, Talapka P, Poles MZ, Hermesz E, Jancsó Z, Katarova Z, Izbéki F, Wittmann T, Fekete É, Bagyánszki M. Gut region-specific diabetic damage to the capillary endothelium adjacent to the myenteric plexus. *Microcirculation* 2012; **19**: 316-326 [PMID: 22296580 DOI: 10.1111/j.1549-8719.2012.00164.x]
13 **Oshitari T**, Brown D, Roy S. SiRNA strategy against overexpression of extracellular matrix in diabetic retinopathy. *Exp Eye Res* 2005; **81**: 32-37 [PMID: 15978252 DOI: 10.1016/j.exer.2005.01.006]
14 **Si YF**, Wang J, Guan J, Zhou L, Sheng Y, Zhao J. Treatment with hydrogen sulfide alleviates streptozotocin-induced diabetic retinopathy in rats. *Br J Pharmacol* 2013; **169**: 619-631 [PMID: 23488985 DOI: 10.1111/bph.12163]
15 **To M**, Goz A, Camenzind L, Oertle P, Candiello J, Sullivan M, Henrich PB, Loparic M, Safi F, Eller A, Halfter W. Diabetes-induced morphological, biomechanical, and compositional changes in ocular basement membranes. *Exp Eye Res* 2013; **116**: 298-307 [PMID: 24095823 DOI: 10.1016/j.exer.2013.09.011]
16 **Roy S**, Bae E, Amin S, Kim D. Extracellular matrix, gap junctions, and retinal vascular homeostasis in diabetic retinopathy. *Exp Eye Res* 2015; **133**: 58-68 [PMID: 25819455 DOI: 10.1016/j.exer.2014.08.011]
17 **McLennan SV**, Kelly DJ, Cox AJ, Cao Z, Lyons JG, Yue DK, Gilbert RE. Decreased matrix degradation in diabetic nephropathy: effects of ACE inhibition on the expression and activities of matrix metalloproteinases. *Diabetologia* 2002; **45**: 268-275 [PMID: 11935159 DOI: 10.1007/s00125-001-0730-4]
18 **Takamiya Y**, Fukami K, Yamagishi S, Kaida Y, Nakayama Y, Obara N, Iwatani R, Ando R, Koike K, Matsui T, Nishino Y, Ueda S, Cooper ME, Okuda S. Experimental diabetic nephropathy is accelerated in matrix metalloproteinase-2 knockout mice. *Nephrol Dial Transplant* 2013; **28**: 55-62 [PMID: 23028104 DOI: 10.1093/ndt/gfs387]
19 **Lu P**, Takai K, Weaver VM, Werb Z. Extracellular matrix degradation and remodeling in development and disease. *Cold Spring Harb Perspect Biol* 2011; **3** [PMID: 21917992 DOI: 10.1101/cshperspect.a005058]
20 **Verma RP**, Hansch C. Matrix metalloproteinases (MMPs): chemical-biological functions and (Q)SARs. *Bioorg Med Chem* 2007; **15**: 2223-2268 [PMID: 17275314 DOI: 10.1016/j.bmc.2007.01.011]
21 **Page-McCaw A**, Ewald AJ, Werb Z. Matrix metalloproteinases and the regulation of tissue remodelling. *Nat Rev Mol Cell Biol* 2007; **8**: 221-233 [PMID: 17318226 DOI: 10.1038/nrm2125]
22 **Van Lint P**, Libert C. Chemokine and cytokine processing by matrix metalloproteinases and its effect on leukocyte migration and inflammation. *J Leukoc Biol* 2007; **82**: 1375-1381 [PMID: 17709402 DOI: 10.1189/jlb.0607338]
23 **Kessenbrock K**, Plaks V, Werb Z. Matrix metalloproteinases: regulators of the tumor microenvironment. *Cell* 2010; **141**: 52-67 [PMID: 20371345 DOI: 10.1016/j.cell.2010.03.015]
24 **Abreu BJ**, de Brito Vieira WH. Metalloproteinase Changes in Diabetes. *Adv Exp Med Biol* 2016; **920**: 185-190 [PMID: 27535260 DOI: 10.1007/978-3-319-33943-6_17]
25 **Kowluru RA**. Role of matrix metalloproteinase-9 in the development of diabetic retinopathy and its regulation by H-Ras. *Invest Ophthalmol Vis Sci* 2010; **51**: 4320-4326 [PMID: 20220057 DOI: 10.1167/iovs.09-4851]
26 **Li SY**, Huang PH, Yang AH, Tarng DC, Yang WC, Lin CC, Chen JW, Schmid-Schönbein G, Lin SJ. Matrix metalloproteinase-9 deficiency attenuates diabetic nephropathy by modulation of podocyte functions and dedifferentiation. *Kidney Int* 2014; **86**: 358-369 [PMID: 24670409 DOI: 10.1038/ki.2014.67]
27 **Xu X**, Xiao L, Xiao P, Yang S, Chen G, Liu F, Kanwar YS, Sun L. A glimpse of matrix metalloproteinases in diabetic nephropathy. *Curr Med Chem* 2014; **21**: 3244-3260 [PMID: 25039784 DOI: 10.2174/0929867321666140716092052]
28 **Brew K**, Nagase H. The tissue inhibitors of metalloproteinases (TIMPs): an ancient family with structural and functional diversity. *Biochim Biophys Acta* 2010; **1803**: 55-71 [PMID: 20080133 DOI: 10.1016/j.bbamcr.2010.01.003]
29 **Arpino V**, Brock M, Gill SE. The role of TIMPs in regulation of extracellular matrix proteolysis. *Matrix Biol* 2015; **44-46**: 247-254 [PMID: 25805621 DOI: 10.1016/j.matbio.2015.03.005]
30 **Wilson AJ**, Furness JB, Costa M. The fine structure of the submucous plexus of the guinea-pig ileum. I. The ganglia, neurons, Schwann cells and neuropil. *J Neurocytol* 1981; **10**: 759-784 [PMID: 7310474 DOI: 10.1007/BF01262652]
31 **Bannerman PG**, Mirsky R, Jessen KR, Timpl R, Duance VC. Light microscopic immunolocalization of laminin, type IV collagen, nidogen, heparan sulphate proteoglycan and fibronectin in the enteric nervous system of rat and guinea pig. *J Neurocytol* 1986; **15**: 733-743 [PMID: 2950210 DOI: 10.1007/BF01625191]
32 **Payette RF**, Tennyson VM, Pomeranz HD, Pham TD, Rothman TP, Gershon MD. Accumulation of components of basal laminae: association with the failure of neural crest cells to colonize the

presumptive aganglionic bowel of ls/Ls mutant mice. *Dev Biol* 1988; **125**: 341-360 [PMID: 3338619 DOI: 10.1016/0012-1606(88)90217-5]

33 **Nagy N**, Barad C, Hotta R, Bhave S, Arciero E, Dora D, Goldstein AM. Collagen 18 and agrin are secreted by neural crest cells to remodel their microenvironment and regulate their migration during enteric nervous system development. *Development* 2018; **145** [PMID: 29678817 DOI: 10.1242/dev.160317]

34 **Kostouros A**, Koliarakis I, Natsis K, Spandidos DA, Tsatsakis A, Tsiaoussis J. Large intestine embryogenesis: Molecular pathways and related disorders (Review). *Int J Mol Med* 2020; **46**: 27-57 [PMID: 32319546 DOI: 10.3892/ijmm.2020.4583]

35 **Hill R**. Extracellular matrix remodelling in human diabetic neuropathy. *J Anat* 2009; **214**: 219-225 [PMID: 19207983 DOI: 10.1111/j.1469-7580.2008.01026.x]

36 **Wedel T**, Holschneider AM, Krammer HJ. Ultrastructural features of nerve fascicles and basal lamina abnormalities in Hirschsprung's disease. *Eur J Pediatr Surg* 1999; **9**: 75-82 [PMID: 10342113 DOI: 10.1055/s-2008-1072217]

37 **Fujiwara N**, Nakazawa-Tanaka N, Miyahara K, Arikawa-Hirasawa E, Akazawa C, Yamataka A. Altered expression of laminin alpha1 in aganglionic colon of endothelin receptor-B null mouse model of Hirschsprung's disease. *Pediatr Surg Int* 2018; **34**: 137-141 [PMID: 28983681 DOI: 10.1007/s00383-017-4180-6]

38 **Nakazawa-Tanaka N**, Fujiwara N, Miyahara K, Nakada S, Arikawa-Hirasawa E, Akazawa C, Urao M, Yamataka A. The effect of laminin-1 on enteric neural crest-derived cell migration in the Hirschsprung's disease mouse model. *Pediatr Surg Int* 2018; **34**: 143-147 [PMID: 29018955 DOI: 10.1007/s00383-017-4181-5]

39 **Livak KJ**, Schmittgen TD. Analysis of relative gene expression data using real-time quantitative PCR and the 2(-Delta Delta C(T)) Method. *Methods* 2001; **25**: 402-408 [PMID: 11846609 DOI: 10.1006/meth.2001.1262]

40 **Jancsó Z**, Bódi N, Borsos B, Fekete É, Hermesz E. Gut region-specific accumulation of reactive oxygen species leads to regionally distinct activation of antioxidant and apoptotic marker molecules in rats with STZ-induced diabetes. *Int J Biochem Cell Biol* 2015; **62**: 125-131 [PMID: 25794426 DOI: 10.1016/j.biocel.2015.03.005]

41 **Sánchez SS**, Genta SB, Aybar MJ, Honoré SM, Villecco EI, Sánchez Riera AN. Changes in the expression of small intestine extracellular matrix proteins in streptozotocin-induced diabetic rats. *Cell Biol Int* 2000; **24**: 881-888 [PMID: 11114237 DOI: 10.1006/cbir.2000.0581]

42 **Johnson PC**. Thickening of the human dorsal root ganglion perineurial cell basement membrane in diabetes mellitus. *Muscle Nerve* 1983; **6**: 561-565 [PMID: 6646159 DOI: 10.1002/mus.880060805]

43 **Hill RE**, Williams PE. Perineurial cell basement membrane thickening and myelinated nerve fibre loss in diabetic and nondiabetic peripheral nerve. *J Neurol Sci* 2004; **217**: 157-163 [PMID: 14706218 DOI: 10.1016/j.jns.2003.09.011]

44 **El-Barrany WG**, Hamdy RM, Al-Hayani AA, Jalalah SM. Electron microscopic study of the myelinated nerve fibres and the perineurial cell basement membrane in the diabetic human peripheral nerves. *Neurosciences (Riyadh)* 2009; **14**: 131-138 [PMID: 21048597]

45 **Yu Q**, Stamenkovic I. Localization of matrix metalloproteinase 9 to the cell surface provides a mechanism for CD44-mediated tumor invasion. *Genes Dev* 1999; **13**: 35-48 [PMID: 9887098 DOI: 10.1101/gad.13.1.35]

46 **Malara A**, Ligi D, Di Buduo CA, Mannello F, Balduini A. Sub-Cellular Localization of Metalloproteinases in Megakaryocytes. *Cells* 2018; **7** [PMID: 30037039 DOI: 10.3390/cells7070080]

47 **Kwan JA**, Schulze CJ, Wang W, Leon H, Sariahmetoglu M, Sung M, Sawicka J, Sims DE, Sawicki G, Schulz R. Matrix metalloproteinase-2 (MMP-2) is present in the nucleus of cardiac myocytes and is capable of cleaving poly (ADP-ribose) polymerase (PARP) in vitro. *FASEB J* 2004; **18**: 690-692 [PMID: 14766804 DOI: 10.1096/fj.02-1202fje]

48 **Aldonyte R**, Brantly M, Block E, Patel J, Zhang J. Nuclear localization of active matrix metalloproteinase-2 in cigarette smoke-exposed apoptotic endothelial cells. *Exp Lung Res* 2009; **35**: 59-75 [PMID: 19191105 DOI: 10.1080/01902140802406059]

49 **Piperi C**, Papavassiliou AG. Molecular mechanisms regulating matrix metalloproteinases. *Curr Top Med Chem* 2012; **12**: 1095-1112 [PMID: 22519442 DOI: 10.2174/1568026611208011095]

50 **Mishra M**, Kowluru RA. Role of PARP-1 as a novel transcriptional regulator of MMP-9 in diabetic retinopathy. *Biochim Biophys Acta Mol Basis Dis* 2017; **1863**: 1761-1769 [PMID: 28478229 DOI: 10.1016/j.bbadis.2017.04.024]

51 **Garcia-Fernandez N**, Jacobs-Cachá C, Mora-Gutiérrez JM, Vergara A, Orbe J, Soler MJ. Matrix Metalloproteinases in Diabetic Kidney Disease. *J Clin Med* 2020; **9** [PMID: 32046355 DOI: 10.3390/jcm9020472]

52 **Zhang L**, He S, Yang F, Yu H, Xie W, Dai Q, Zhang D, Liu X, Zhou S, Zhang K. Hyperoside ameliorates glomerulosclerosis in diabetic nephropathy by downregulating miR-21. *Can J Physiol Pharmacol* 2016; **94**: 1249-1256 [PMID: 27704873 DOI: 10.1139/cjpp-2016-0066]

53 **Wang J**, Gao Y, Ma M, Li M, Zou D, Yang J, Zhu Z, Zhao X. Effect of miR-21 on renal fibrosis by regulating MMP-9 and TIMP1 in kk-ay diabetic nephropathy mice. *Cell Biochem Biophys* 2013; **67**: 537-546 [PMID: 23443810 DOI: 10.1007/s12013-013-9539-2]

54 **McLennan SV**, Fisher E, Martell SY, Death AK, Williams PF, Lyons JG, Yue DK. Effects of glucose on matrix metalloproteinase and plasmin activities in mesangial cells: possible role in diabetic nephropathy. *Kidney Int Suppl* 2000; **77**: S81-S87 [PMID: 10997695 DOI:

10.1046/j.1523-1755.2000.07713.x]
55 **McLennan SV**, Kelly DJ, Schache M, Waltham M, Dy V, Langham RG, Yue DK, Gilbert RE. Advanced glycation end products decrease mesangial cell MMP-7: a role in matrix accumulation in diabetic nephropathy? *Kidney Int* 2007; **72**: 481-488 [PMID: 17554258 DOI: 10.1038/sj.ki.5002357]
56 **Kim KM**, Chung KW, Jeong HO, Lee B, Kim DH, Park JW, Kim SM, Yu BP, Chung HY. MMP2-A2M interaction increases ECM accumulation in aged rat kidney and its modulation by calorie restriction. *Oncotarget* 2018; **9**: 5588-5599 [PMID: 29464020 DOI: 10.18632/oncotarget.23652]
57 **Mohammad G**, Siddiquei MM. Role of matrix metalloproteinase-2 and -9 in the development of diabetic retinopathy. *J Ocul Biol Dis Infor* 2012; **5**: 1-8 [PMID: 23833698 DOI: 10.1007/s12177-012-9091-0]
58 **Kowluru RA**, Mishra M. Regulation of Matrix Metalloproteinase in the Pathogenesis of Diabetic Retinopathy. *Prog Mol Biol Transl Sci* 2017; **148**: 67-85 [PMID: 28662829 DOI: 10.1016/bs.pmbts.2017.02.004]
59 **Drankowska J**, Kos M, Kościuk A, Marzęda P, Boguszewska-Czubara A, Tylus M, Święch-Zubilewicz A. MMP targeting in the battle for vision: Recent developments and future prospects in the treatment of diabetic retinopathy. *Life Sci* 2019; **229**: 149-156 [PMID: 31100326 DOI: 10.1016/j.lfs.2019.05.038]
60 **Han SY**, Jee YH, Han KH, Kang YS, Kim HK, Han JY, Kim YS, Cha DR. An imbalance between matrix metalloproteinase-2 and tissue inhibitor of matrix metalloproteinase-2 contributes to the development of early diabetic nephropathy. *Nephrol Dial Transplant* 2006; **21**: 2406-2416 [PMID: 16728425 DOI: 10.1093/ndt/gfl238]
61 **Medina C**, Radomski MW. Role of matrix metalloproteinases in intestinal inflammation. *J Pharmacol Exp Ther* 2006; **318**: 933-938 [PMID: 16644899 DOI: 10.1124/jpet.106.103465]

Published by **Baishideng Publishing Group Inc**
7041 Koll Center Parkway, Suite 160, Pleasanton, CA 94566, USA
Telephone: +1-925-3991568
E-mail: bpgoffice@wjgnet.com
Help Desk: https://www.f6publishing.com/helpdesk
https://www.wjgnet.com